System Study on Hydrothermal Gasification Combined with a Hybrid Solid Oxide Fuel Cell Gas Turbine

Richard Toonssen, P.V. Aravind, Gerton Smit, Nico Woudstra, Adrian Verkooijen

Fuel Cells

System Study on Hydrothermal Gasification Combined with a Hybrid Solid Oxide Fuel Cell Gas Turbine

Journal:	*Fuel Cells*
Manuscript ID:	fuce.200900188.R1
Wiley - Manuscript type:	Original Research Paper
Date Submitted by the Author:	15-Jan-2010
Complete List of Authors:	Toonssen, Richard; TU-Delft, Process and Energy Aravind, P.V.; TU-Delft, Process and Energy Smit, Gerton; Gensos V.O.F Woudstra, Nico; TU-Delft, Process and Energy Verkooijen, Adrian; TU-Delft, Process and Energy
Keywords:	Cycle Tempo, Exergy analysis, Hydrothermal biomass gasification, Modelling, Solid Oxide Fuel Cell, SOFC-GT hyrbid system

System Study on Hydrothermal Gasification Combined with a Hybrid Solid Oxide Fuel Cell Gas Turbine

R. Toonssen[1*], P.V. Aravind[1], G. Smit[2], N. Woudstra[1], A. H. M. Verkooijen[1]

[1] Delft University of Technology, Faculty of Mechanical, Marine and Material Engineering, Process and Energy Department, Section Energy Technology, Leeghwaterstraat 44, 2628CA Delft, The Netherlands
[2] GENSOS V.O.F., Wijdense Spaansweg 57, 1764GK Breezand, The Netherlands

Recieved:

[*] Corresponding author, R.Toonssen@TUDelft.NL

Abstract

The application of wet biomass in energy conversion systems is challenging, since in most conventional systems the biomass has to be dried. Drying can be very energy intensive especially when the biomass has a moisture content above 50 wt% on a wet basis. The combination of hydrothermal biomass gasification and a solid oxide fuel cell (SOFC) gas turbine (GT) hybrid system could be an efficient way to convert very wet biomass into electricity. Therefore, thermodynamic evaluation of combined systems with hydrothermal gasification units and SOFC-GT hybrid units has been performed. Three hydrothermal gasification cases have been evaluated; one producing mainly methane, a second one producing a mixture of hydrogen and methane and the last one producing mainly hydrogen. These three gasification systems have been coupled to the same SOFC-GT hybrid system. All the integrated systems have electrical exergy efficiencies around 50%, therefore the combination of supercritical water gasification and SOFC-GT hybrid systems seems promising. The overall system performance depends for a large part on the liquid gas separation. Further research is required for finding out the optimal separation conditions.

Keywords: Cycle-Tempo, Exergy Analysis, Hydrothermal Biomass Gasification, Modelling, SOFC-GT Hybrid System

1. Introduction

Increasing concerns about the environmental impacts of fossil fuel consumption and their depletion lead to a rising attention towards more sustainable sources of energy. Biomass is one of the considered sustainable energy sources, due to its carbon dioxide neutrality. Especially, biomass waste and residual biomass streams can be used for energy conversion processes. Many of the modern energy conversion systems convert the biomass first into a secondary energy carrier, before it is converted into electricity. This is because the biomass is usually in a form, which is hard to convert into electricity directly. For instance, manure is usually very wet and cannot be combusted without being dried first. In hydrothermal gasifiers, it is possible to convert wet biomass into a methane or hydrogen rich gas. The gas produced in hydrothermal gasification is relatively clean compared to gas coming from conventional gasification processes. Therefore, simple gas cleaning is sufficient when compared with conventional gasification systems. The methane or hydrogen rich gas produced in hydrothermal gasifiers can be used to produce electricity.

The solid oxide fuel cell (SOFC) is an electrochemical device, which can convert the chemical energy in fuel into electricity in an efficient manner. Common fuels for solid oxide fuel cells are hydrogen, methane, or synthesis gas. When operated at elevated pressures, the SOFC can be combined with a gas turbine (GT), to obtain a very efficient power plant.

The combination of biomass gasification with SOFC-GT hybrid systems is getting significant attention from the scientific community [1-11]. All these studies focus on the gasification of relatively dry biomass combined with either SOFCs or SOFC-GT hybrid systems. The combination of super critical water gasification and fuel cells is a new concept. There is one study performed by Li et al. [12], where a tubular SOFC is tested with simulated syn-gas assumed to be coming from supercritical water gasification.

In this paper, results from thermodynamic evaluations of power plants with hydrothermal gasification systems coupled with SOFC-GT systems are presented. Three different hydrothermal gasification options have been evaluated; one operates at a temperature of 673 K for the production of mainly methane, the second operates at 773 K for the production of a mixture of methane and hydrogen and the last one operates at 873 K for the production of mainly hydrogen. The three types of gasifiers have been coupled to a solid oxide fuel cell- gas turbine hybrid system. Exergy analyses of the complete systems were performed.

2. Description of Subsystems

The considered systems are divided into three sub-systems, the hydrothermal gasification system, the solid oxide fuel cell system and the gas turbine system. The sub-systems are described in the following sections, respectively.

2.1. Hydrothermal Gasification

Hydrothermal gasification is also known as subcritical or supercritical water gasification. With this technique, a primary fuel is converted into a secondary fuel in an aqueous medium at temperatures above or around 473 K and a sufficient high pressure to keep the water in a liquid or super critical state [13]. This gasification technique has several advantages over conventional gasification techniques:

- Ability to use very wet biomass sources (>80%), like manure
- High gasification efficiency at relative low temperatures
- Low formation of tars and chars

Hydrothermal biomass gasification can be divided into three main types [14, 15]:

(i) Aqueous phase reforming, compounds originating from biomass (for instance, glucose, sorbitol, glycerol) are gasified at around 488-543 K to mainly hydrogen and carbon dioxide in the presence of a heterogeneous catalyst.

(ii) Catalyzed (near)-critical gasification, biomass is gasified in the presence of a catalyst to mainly methane and carbon dioxide at either around 623 K in the liquid phase or around 673 K in the supercritical state.

(iii) Super critical water gasification, biomass compounds are gasified to mainly hydrogen and carbon dioxide with or without a catalyst at temperatures around 873-973K.

In hydrothermal gasification the idea is to benefit from the special properties of near critical or supercritical water [14]. Water from ambient to supercritical conditions changes its character from a solvent for ionic species to a solvent for non-ionic species [16]. Also the electrochemical properties of water change from ambient conditions. The pH values decreases by three units, providing more hydronium ions for acid catalyzed reactions [16]. The reactivity of water increases near the critical point with as well as without catalyst [16]. At near critical and supercritical conditions water and gasses like O_2, N_2, NH_3, CO, CO_2 are completely miscible and the solubility for inorganic compounds in water decreases [15].

In hydrothermal gasification, water is not only used as a solvent, but also as a reaction partner. Biomass is relatively fast hydrolysed in near or supercritical water resulting in a rapid degradation of the polymeric structure of the biomass into a mixture of sugars [14]. The sugars are further converted as indicated in reactions (1) and (2).

$$C_6H_{12}O_6 + 6H_2O \rightarrow 6CO_2 + 12H_2 \qquad (1)$$

$$C_6H_{12}O_6 \rightarrow 3CH_4 + 3CO_2 \qquad (2)$$

In these reactions, the sugars are represented as glucose. The reactions (1) and (2) are also relatively fast resulting in a gas at relatively low temperature compared to the “dry process” [14, 15]. The high solubility of the intermediates in the reaction medium significantly inhibits tar and coke formation [14, 15]. After the reaction and cooling carbon dioxide is mainly dissolved in the water, due to its high solubility at elevated pressures. The pressurized gas separated from the liquid phase has a relatively low CO_2 content, hence, a high heating value [14].

A major disadvantage of hydrothermal gasification is the large amount of water which needs to be heated. The heat required to reach e.g. 873 K can exceed the energy content of the applied biomass [14]. Therefore, the application of a heat recovery heat exchanger is required and the efficiency of the heat exchanger is very important.

Supercritical water gasification (SCWG) has special material requirements for the reactor, since in super critical water gasification both the temperature and pressure are high [14]. One of the important problems in hydrothermal gasification is reactor plugging [14, 17, 18]. This is caused by the formation of inorganic salts, which precipitate during the gasification process. The salts can also have deteriorating effect on catalysts [16].

In this paper three cases are considered; the main difference between these cases is the type of hydrothermal gasification employed.

- Case 1, the hydrothermal gasification operates at a temperature of around 673 K, a pressure of 34 MPa and uses a catalyst (activated carbon). This system produces mainly methane and carbon dioxide using mainly reaction (2)
- Case 2, operates at a temperature of approximately 773 K, a pressure of 34 MPa and without a catalyst. The product of this system is a mixture of hydrogen, methane and carbon dioxide using both reaction (1) and (2)
- Case 3, operates at 873 K, a pressure of 24 MPa and also without catalyst. This system produces mainly hydrogen and carbon dioxide using mainly reaction (1).

The gas produced during the SCWG is separated from the water by flashing. The produced gas contains some impurities, like hydrochloric acid and hydrogen sulphide. These compounds need to be removed before the gas is fed to the SOFC-GT hybrid system. The SOFC-GT is considered as sensitive towards poisoning by hydrochloric acid and hydrogen sulphide when they are present in excessive quantities, which results in performance deterioration of the systems. Before the removal of hydrochloric acid and hydrogen sulphide, superheated steam is added to the gas to increase the moisture content of the gas and to prevent carbon deposition in the acid gas removal units. Hydrochloric acid is removed by adsorption on sodium carbonate and hydrogen sulphide is removed by adsorption on zinc oxide. Both adsorption processes are performed in packed beds.

The technology of hydrothermal biomass gasification is still in its development stage.

There is some experimental data available, but the results are not compared to experimental results. Most of the experimental data available is based on model compounds, like glucose, and very limited data on actual biomass or in this case manure.

2.2. Solid oxide fuel cell system

As it is in the case of hydrothermal gasification, the SOFC technology is also still in a development stage. The solid oxide fuel cell considered in this work is based on Ni/GDC anodes and lanthanum strontium manganite (LSM) cathodes at temperatures above 1173K. No relevant data is available about stack performance using bio-syngas. Some reports on cell performance using bio-syngas are available [1, 19]. Based on these reports, data necessary for system calculations have been assumed. These assumptions are for the values of different parameters, like fuel cell resistance and current density.

2.3. Gas turbine and heat recovery system

The gas turbine system does not represent any commercially available gas turbine. The isentropic and mechanical efficiencies are chosen such that, they could represent a well matched gas turbine. The anode gas and cathode gas coming from the fuel cell are partially recycled to the inlet of the fuel cell. The residual gasses are fed to the combustion chamber of the gas turbine. All these units operate at elevated pressure. The flue gasses from the combustion are expanded in the turbine. The turbine exhaust gasses are used to pre-heat the air for the fuel cell.

The flue gasses coming from the gas turbine are mixed with the flue gasses coming form the gasification part. After the mixing of the flue gasses, it is still possible to extract heat from the flue gasses. This is included as a heat sink which represents a heat consumer. The recovered heat can be applied for various purposes. The flue gasses are released in the atmosphere through a stack at a temperature of 383 K.

3. Modelling

For the modelling of hydrothermal gasification systems combined with the SOFC-GT hybrid system, the flow sheeting program Cycle-Tempo [20] is used. This flow sheeting program is especially designed for the evaluation of energy conversion systems. For the flash calculations required in the systems, the computer program Aspen Plus [21] is used. In this section, a description of the model and of the modelling principles applied is given. First the gasification model is discussed and then the SOFC-GT hybrid system. Finally, the used assumptions and model input are presented.

3.1. Hydrothermal gasification of manure

The manure used in this system study is assumed to be a mixture of cow manure and pig manure. The dry ash free (daf) composition of the manure is taken from Phyllis [22], a database of compositions of biomass and waste. The used values are given in Table 1. These values in the wet composition are based on the assumption of a moisture content of 80 wt% on wet basis. The calculated values of the wet manure can also be found in Table 1.

In Fig. 1, the flow sheet of the hydrothermal gasification of manure is given. For modelling purposes the manure is put into the model as a gas stream. The compression of the manure is modelled as a sink (no. 2). The output pressure and output temperature are set to the values calculated for the compression of liquid water with an isentropic efficiency of 60% and a mechanical efficiency of 90%. The required power input for the pump is also included in the calculations. This approach is used since Cycle-Tempo overestimated the power input requirement of the compression as Cycle-Tempo could not handle the fuel as a liquid.

The hydrothermal gasification is modelled with single gasifier unit (no. 5); this unit calculates the outgoing gas composition via minimization of the Gibbs energy. For a first estimation of the gas composition coming from the SCWG, Gibbs energy minimization has shown to give good overall predictions for the gas composition [23, 24].

The salts which are formed during the gasification are removed in a separator (no. 6). Some of the heat is then recuperated in heat exchanger (no. 3).

To separate the product gas from the water the pressure is released to flash pressure (sink no. 7) and the fluid is cooled to 298 K with cooling water (heat exchanger no. 8). The mixture is flashed separating the gas from the

liquid. The liquid stream is flashed to atmospheric pressure (separator no. 71), to release the dissolved gasses from the liquid water. These released gasses are combusted in a combustor (no. 72) to provide additional heat to the process (heat exchangers no. 4 and 11).

For the flash calculations, a separate Aspen model is used, since in Cycle-Tempo it is not possible to do this type of flash calculations. The thermodynamic model used for these flash calculations is Redlich-Kwong-Soave model with modified Huron-Vidal mixing rules [25]. From the flash calculations the separation ratios are determined for the two separators which represent the flashes (no.9 & 71) in the Cycle-Tempo model. The separation factors for hydrochloric acid are not calculated by Aspen, since Aspen is not able to do the calculations on ioninc compounds with the Redlich-Kwong-Soave with modified Huron-Vidal mixing rules equations of state model. The solubility of hydrochloric acid is expected to be high, so the separation factors of 95% for the first flash and 75% for the second flash are chosen.

The gas released by the first flash (separator no. 9) is the product which is used later as fuel for the fuel cell. This gas still contains small amounts of hydrochloric acid and hydrogen sulphide. These small amounts need to be removed, since they will have a deteriorating effect on the SOFC-GT hybrid system. Before the hydrogen sulphide and hydrochloric acid is removed, steam is added to the gas in order to prevent carbon formation in the removal system. The superheated steam is produced in a boiler (no. 73) using the hot flue gasses coming from the combustor.

The hydrochloric acid is removed in packed bed with sodium carbonate and hydrogen sulphide is removed from the gas in a packed bed with zinc oxide. This is modelled as a separator (no. 13) with a pressure drop which is assumed to remove all the hydrochloric acid and hydrogen sulphide from the gas. The gas is then heated in a heat exchanger (no. 14) with the hot flue gas coming from the combustor (no 72).

3.2. Solid Oxide Fuel Cell Gas Turbine Hybrid System

In Fig. 2 the flow sheet for the SOFC-GT hybrid system is given. The fuel gas coming from the gasification section is mixed with a recycled stream from the fuel cell anode before it enters the fuel cell (no. 16). The fuel cell is modelled as a direct internal reforming (DIR) solid oxide fuel cell. The anode gas entering the fuel cell is brought to its chemical equilibrium by means of Gibbs minimization calculations. Then the cell voltage V, active cell area, the current flow I and the electrical power output P_e are calculated by the model. The fuel mass flow into the fuel cell is related to the current flow as indicated in equation (3).

$$I = \frac{\phi_{m,a,in}}{M_a} 2F(y^0_{H_2} + y^0_{CO} + 4y^0_{CH_4})U_f \qquad (3)$$

Here, y^0_i are the concentrations of the different components at the inlet, M_a is the molar mass of the anode gas, F is the Faraday constant and U_f is the fuel utilization.

The temperature and pressure are supposed to be constant during the process. The mass flow of oxygen from the cathode to the anode is calculated based on the current flow. An energy balance is used to calculate the air flow through the fuel cell, since the temperature at the outlet is given. For the calculation of the cell voltage, the current density and power output a one dimensional model is used. This means that the temperature, pressure and composition are supposed to be constant in a cross-section, perpendicular to the flow of fuel through the fuel cell. The local reversible cell voltage $V_{rev,x}$, the local current density i_x and the local concentrations y_x(H_2, CO, CO_2, CH_4 and H_2O) are calculated. For the cross-section the reversible cell voltage $V_{rev,x}$ is determined with the Nernst equation assuming ideal gas:

$$V_{rev,x} = V^0_{rev} + \frac{RT}{2F} \ln\left(\frac{y^{0.5}_{O_2,c} y_{H_2,a}}{y_{H_2O,a}} \times p^{0.5}_{cell} \right) \qquad (4)$$

Where V^0_{rev} is the standard reversible voltage for hydrogen, R the universal gas constant, T is the temperature, y is the mole fraction at the cross-section and p_{cell} is the pressure. It is assumed that the voltage losses on the level of the electrodes are negligible in the x-direction. This means that the cell voltage is supposed to be constant over the fuel cell. So, the voltage loss ΔV_x can be calculated using the following equation:

$$\Delta V_x = V_{rev,x} - V \qquad (5)$$

Where ΔV_x is the voltage loss. The current density can then be calculated with:

$$i_x = \frac{\Delta V_x}{R_{eq}} \qquad (6)$$

Here R_{eq} is the equivalent fuel cell resistance.

Over the whole fuel cell these quantities are connected with the following equation:

$$\frac{I}{A} = \frac{U_f}{R_{eq} \int_0^{U_F} \frac{d\xi}{(V_{rev,x} - V)}} \qquad (7)$$

Here, I is the total current, A is the fuel cell area and ξ is the dimensionless reaction coordinate. With the current and voltage known the power output can be calculated.

The residual fuel leaving the fuel cell is combusted in a combustor (no. 18). The hot flue gasses are then expanded in a turbine (no. 19) which is connected to a generator through a shaft. The enthalpy of the outlet is calculated using equation (8), for the compressor equation (9) is used.

$$h_{out} = h_{in} - \eta_i (h_{in} - h_{out,s}) \quad (8)$$

$$h_{out} = h_{in} + \frac{(h_{out,s} - h_{in})}{\eta_i} \quad (9)$$

In these equations, h_{out} is the specific enthalpy of the outlet, h_{in} the specific enthalpy of the inlet, η_i the isentropic efficiency and $h_{out,s}$ is the specific enthalpy of the gas when isentropically expanded. When the enthalpy change is known, the power output can be determined with the mass flow.

The flue gasses are used in a recuperator (no. 20) to pre-heat the cathode air. Finally the flue gasses are mixed with the flue gas from the gasification plant and a part of the heat is recovered in a heat sink (no. 23). This heat could be used to produce even more electricity, for example, with an organic rankine cycle. After this, the gas is released to the environment through a stack (no. 21).

3.3 Assumptions and model input

Several general assumptions have been made for the models:

- Steady state
- No fouling in the equipment
- No catalyst deactivation
- All processes are adiabatic
- The heat exchangers are operated in counter current flow

The input values for the hydrothermal gasification of the different systems are given in Table 2. In Table 3, the input values for the SOFC-GT hybrid system are given. For both tables, the temperatures (T) are given in °C, the pressures (p) in bar, the mass flow (ϕ_m) in kg s^{-1}, the equivalent fuel cell resistance (R_{eq}) in Ω m^2 and the current density (i) in A m^{-2}. The full description of the symbols is given in the list of symbols.

Cycle Tempo can perform exergy calculations. The exergy of all flows considered in the flow sheet is calculated based on previously calculated temperatures, pressures and chemical composition. The thermo-mechanical (physical) exergy and chemical exergy are calculated separately.

The thermo-mechanical exergy Ex_{tm} is calculated using equation (10).

$$Ex_{tm} = (h - h_0) - T_0 (s - s_0) \quad (10)$$

Here, h is the enthalpy of a stream, s is the entropy of a stream, h_0 is the enthalpy of a stream at reference conditions, s_0 is the entropy of a stream at reference conditions and T_0 is the temperature at reference conditions.

For the calculation of the chemical exergy, a definition of the environment is required. The composition of the environment in the calculation is given in Table 4, which is the composition of air saturated with water vapour as specified by Baehr [26], but at an environmental temperature of 288 K and pressure of 101325 Pa. The chemical exergy Ex_{ch} is calculated using equation (11).

$$Ex_{ch} = \sum_i y_i ex_{0,i} + RT_0 \sum_i y_i \ln y_i \quad (11)$$

Here, y_i is the molar fraction of component i, $ex_{0,i}$ is the standard chemical exergy of component i which is based on the reference environment and T_0 is the reference temperature,

The overall exergy Ex is calculated using the following relation:

$$Ex = \phi_{mol} (Ex_{tm} + Ex_{ch}) \quad (12)$$

Where, ϕ_{mol} is the molar flow.

Chlorine, sulphur and the elements in the ash are not defined in the chemical composition of the environment. Therefore, the components containing these elements are assumed to have zero exergy. Since the concentrations of these elements in the biomass are very low this assumption would result only in a negligible error.

Energy efficiencies are based on the Lower Heating Value (LHV) of the fuel. The exergy efficiency is generally defined as follows.

$$\eta_{ex} = \frac{\sum Ex_{products}}{\sum Ex_{source}} \quad (13)$$

Where $Ex_{products}$ is the exergy of the flows which are considered to be products going out of the systems, Ex_{source} is the exergy of the flows which are considered to be necessary for making the product going into the system. Further specification of the $Ex_{product}$ and Ex_{source} is necessary in order to calculate system efficiencies. In this paper the electrical exergy efficiency ($\eta_{ex,el}$) is defined as:

$$\eta_{ex,el} = \frac{\sum P_{el.out} - \sum P_{el,in}}{Ex_{fuel,in}} \quad (14)$$

Here is $P_{el,out}$ the gross electrical output of the system, $P_{el,in}$ the electrical power input in the system (auxiliary power) and $Ex_{fuel,in}$ is the exergy of the fuel put into the system.

4. Results and discussion

The mixture of pig and cow manure enters the system with a mass flow of 0.28 kg/s at environmental conditions. This stream is pressurized to a pressure of 35 MPa for cases 1 and 2. For case 3 the manure is pressurized to a pressure of 25 MPa. The pressurization results in power consumption of the pump of 17.83 kW for cases 1 and 2, for case 3 this is 12.75 kW. After the pressurization, the fluid is heated in heat exchangers to process conditions and then gasified. The precipitated solid salts are removed and the fluid is cooled by heat exchanging with the pressurized feed. Then some pressure is released till a pressure of 15.3 MPa and the fluid is further cooled. In Table 5, the composition of the resulting fluid (pipe 10) for the different systems is given.

The composition of pipe 10 is entered into the Aspen flash model to determine the separation factors. These separation factors are given in Table 6 for every case. The chosen separation factors for hydrochloric acid will hardly influence the calculations since the concentrations are low. In this model it is not important for determining the system performance, since it is assumed that the chlorine removal bed will adsorb all the residual chlorine. When designing an actual system to be built; it is important to know how much chlorine will be in the gas after the flash. Especially, when dimensioning the chlorine removal system. Hydrochloric acid may have a detrimental effect on the solid oxide fuel cell. Chlorine is a bit tricky, its influence is not that clearly known.

For case 3, a higher pressure is used in the first flash. This is done to increase the amount of combustibles dissolved in the water. These combustibles are used after the second flash for the generation of heat for the process. When the same pressure was used as in the cases 1 & 2, the heat generation was not sufficient for the process.

The resulting gas composition for pipe 11 can be found in Table 5. The gas is further expanded to 6.9 bar and then heated in the following heat exchanger to 673 K before steam is added. In case 1, 0.008 kg s^{-1} steam is added with a temperature of 673 K and a pressure of 6.8 bar. In cases 2 and 3, 0.005 kg s^{-1} steam is added at same conditions as in case 1. Since the gas in case 1 is methane rich, more steam is required. This steam is also used in the reforming process in the SOFC downstream. The steam is added to prevent carbon formation in the sulphur and chlorine removal as well as in the SOFC. The composition of the gas sent to the SOFC-GT hybrid system (pipe 16) is given in Table 5.

Before the gas enters the anode of the fuel cell, it is mixed with the anode recycle stream. The mixture enters the fuel cell at 1173 K. Air extracted from the environment is compressed in the compressor of the gas turbine and heated in the recuperator, before it is mixed with the cathode recycle stream. The air mixture enters the cathode of the fuel cell at a temperature of 1173 K. Part of the anode off-gas is recycled as well as a part of the cathode off-gas is recycled, the recycle ratios for every case can be found in Table 7. The residual off-gasses enter a combustor where the residual fuel in the anode off-gas is combusted. The hot flue gas is expanded in the turbine. In Table 7, results can be found of the SOFC/GT hybrid system for the different cases.

In Table 8, an overview of the power production and the efficiencies of the different systems are given.

As can be seen in Table 8, the net electrical performances of the three cases do not deviate much from each other. The electrical exergy efficiency is around 50%, which is comparable to the efficiency of conversion systems based on dry biomass, like in refs. [2, 11]. When wet biomass is applied in systems for dry biomass, the biomass has to be dried first. The drying will reduce the performance of the systems based on dry biomass.

In order to get an overview where the exergy losses within the system occur, an exergy flow diagram has been created for each case. In these diagrams, the losses are indicated by the gray areas. In Fig. 3, the exergy flow diagrams for the three cases are given. The unit numbers which are included in the different system sections as indicated in Fig. 3 are given in Table 9.

From Fig. 3, it can be seen that the gasification section has the largest losses in the whole system. The losses for the gasification are in case 1 larger than for cases 2 &3. The losses are mainly caused by the irreversibilities in the gasifier (unit 5). The chemical exergy of the stream leaving the gasifier is smaller for case 1 than for the

other two cases and the chemical exergy of the input stream is for the three cases the same. This chemical exergy is lost for a large part. Since the loss of exergy should be minimized, cases 2 & 3 are preferred. Other larger contributors in losses of the gasification section are the heat exchangers (unit 3 & 8) and the combustor (unit 72).

The losses in the gas cleaning section of case 2 are significantly lower than for the other two systems. The losses in this section are dominated by the heat exchangers and the boiler. The cause of these losses can be clearly shown by heat-temperature diagrams of the heat exchangers (units 11 & 14) and the boiler (unit 73) for every case. In Fig. 4, the heat-temperature diagrams of units 11, 14 and 73 for the different cases are given.

The slope of the hot fluid temperature line is steeper in case 2 (14.1 K kW^{-1}) than for the other two cases (for case 1: 12.7 K kW^{-1} and for case 3: 9.6 K kW^{-1}). In the other two cases more flue gas is formed in combustor (unit 72), resulting in a larger mass flow. The amount of combustibles going to the combustor is determined by the flash conditions, and that determines the amount of flue gas that is produced. The air factor is for every system the same. Also, the temperature differences between the hot fluid and cold fluids are smaller for case 2 than for the other cases. This is represented by the shaded area in Fig. 4.

The power output of the fuel cell in case 3 is lower than in the other systems. This is partly caused by the fact that more anode gas is recycled than in the other systems. The recycling has a diluting effect on the fuel, resulting in a lower fuel cell output. The lower performance of the fuel cell is partly compensated by the higher output of the gas turbine. The air flow through the fuel cell is higher than in the other cases, because the fuel cell requires more cooling due to lower methane fraction and higher hydrogen fraction in the fuel.

For case 1, the losses for the gas turbine are smaller than in the other systems. This is partly caused by the amount of air required in the SOFC-GT hybrid system. The fuel cell is cooled by the cathode air flow. If the amount of hydrogen in fuel increases, the fuel cell requires more cooling, because less heat is extracted by the internal reforming. The increased mass flow of air causes an increase of the losses in the air compressor, air recycle blower, turbine and mixing points.

Case 3 has a larger heat production than the cases 1 &2. Since case 3 has the largest mass flow of flue gas coming from the combustor.

The two flue gas streams coming from the gasification section and from the gas turbine are mixed to make it easier to extract heat from it. The heat is extracted by a heat consumer, which cools the flue gas to a temperature of 383 K. This value is chosen to prevent condensation of the water in the flue gas. The type of heat consumer is not further researched, many options are available, for instance, an organic rankine cycle for the production of additional electricity, steam production for other process, production of hot water for district heating, etc.

The most determining factor for the performance of the whole system is the flash conditions of the first flash vessel. The flash conditions determine the amount of gas and the composition of the gas. The solubility of the different components in water depends on the pressure. The secondary flash is used to release the dissolved compounds from the water, which results in a combustible gas. It is possible to optimize the flash conditions in such a way that the maximal amount of gas for the fuel cell is produced and still enough heat can be produced from the gas released in the second flash to support the processes. This optimization is not performed, and is considered as a future research topic. The current flash conditions deliver almost similar mass flows of gas towards the gas cleaning section and SOFC-GT system.

5. Conclusions

The coupling of hydrothermal biomass gasification and a SOFC-GT hybrid system has been thermodynamically evaluated by modelling several systems in Cycle Tempo. The biomass used in this study is a mixture of pig and cow manure with a moisture content of 80 wt% on a wet basis. Three different types of hydrothermal gasification have been modelled and combined with a SOFC-GT hybrid system. Case 1 is based on catalytic gasification at a temperature of around 673K and a pressure of 34 MPa; this results in a producer gas of mainly methane, carbon dioxide and a relatively small amount of hydrogen. Case 2 is based on non-catalytic gasification at a temperature of 773K and a pressure of 34 MPa resulting in a mixture of hydrogen, methane and carbon dioxide. Case 3 is based on non-catalytic hydrothermal gasification at a temperature of 873K and a pressure of 24 MPa resulting in a hydrogen rich gas. The coupled SOFC-GT hybrid is kept identical for every system. The electrical exergy efficiency for the cases 1, 2 and 3 are 49.8%, 51.8% and 49.6%, respectively. These efficiency values are reasonably comparable with previously reported efficiencies for SOFC-GT systems combined with conventional gasification techniques based on dry biomass. The combination of hydrothermal gasification and SOFC-GT hybrid systems seems very promising especially for wet biomass streams.

The non-catalytic hydrothermal gasification processes of cases 2 & 3 are preferred, since these processes have lower chemical exergy losses in the gasification than case 1.

The conditions of the flash used for separating the gas from the liquid have a large influence on the performance of the system because it influences the amount of combustibles dissolved in the liquid. Further study into the flash conditions is required to optimize the system.

List of Symbols

λ	Air factor
η	Efficiency / %
η_{ex}	Exergy efficiency / %
$\eta_{ex,el}$	Electrical exergy efficiency / %
ΔH_{out}	Enthalpy change / kJ kg^{-1}
η_i	Isentropic efficiency / %
ϕ_m	Mass flow / kg s^{-1}
$\phi_{m,a,in}$	Mass flow at inlet of anode / kg s^{-1}
ϕ_{mol}	Molar flow / mol s^{-1}
ξ	Dimensionless reaction coordinate
Δp	Pressure drop / bar
Δp_1	Pressure drop for primary stream / bar
Δp_2	Pressure drop for secondary stream / bar
Δp_{an}	Pressure drop at the anode of a fuel cell / bar
Δp_{cat}	Pressure drop at the cathode of a fuel cell / bar
Δp_h	Pressure drop at hot side of a heat exchanger / bar
Δp_l	Pressure drop at cold side of a heat exchanger / bar
ΔV_x	Voltage loss / V
A	Active cell area / m^2
DCAC	Efficiency of the DC to AC conversion / %
$ex_{0,i}$	Standard chemical exergy of component i / kJ mol^{-1}
Ex	Exergy of a stream / kW
Ex_{tm}	Thermo-mechanical exergy / kJ mol^{-1}
Ex_{ch}	Chemical exergy / kJ mol^{-1}
$Ex_{fuel,in}$	Exergy of the fuel input / kW
$Ex_{product}$	Exergy content of the products / kW
Ex_{source}	Exergy content of the sources / kW
F	Faradays' constant
h	Enthalpy of a stream / kJ mol^{-1}
h_0	Enthalpy of a stream at reference conditions / kJ mol^{-1}
h_{in}	Enthalpy of a stream at the inlet / kJ mol^{-1}
h_{out}	Enthalpy of a stream at the outlet / kJ mol^{-1}
$h_{out,s}$	Enthalpy of a stream at the outlet in case of isentropic compression/expansion / kJ mol^{-1}
i	Current density / A m^{-2}
I	Current / A
y_i^0	Molar fraction of component i at the inlet
$y_{i,c}$	Molar fraction of component i at the cathode
$y_{i,a}$	Molar fraction of component i at the anode
M_a	Molar mass anode gas / kg mol^{-1}
$P_{el,in}$	Electrical power input / kW
$P_{el,out}$	Electrical power output / kW
p_{cell}	Fuel cell pressure / bar
p_{out}	Outlet pressure / bar
$p_{out,2}$	Outlet pressure of the secondary stream / bar
PR	Pressure ratio
p_{react}	Reaction pressure / bar
R	Universal gas constant
R_{eq}	Equivalent fuel cell resistance / Ω m^2
s	Entropy of a stream / kJ mol^{-1} K^{-1}
s_0	Entropy of a stream at reference conditions / kJ mol^{-1} K^{-1}
T_0	Reference temperature / °C
T_{fc}	Fuel cell temperature / °C
$T_{in,2}$	Inlet temperature secondary stream / °C
$T_{in,an}$	Inlet temperature at the anode of a fuel cell / °C

$T_{in,cat}$	Inlet temperature at the cathode of a fuel cell / °C
T_{out}	Outlet temperature / °C
$T_{out,2}$	Outlet temperature of the secondary stream / °C
$T_{out,est}$	Estimate outlet temperature / °C
$T_{out,h}$	Temperature of the outlet at the hot side of a heat exchanger / °C
T_{react}	Reaction temperature / °C
U_f	Fuel utilization
V	Cell voltage / V
$V_{rev,x}$	Reversible cell voltage / V
$V^0_{rev,x}$	Standard reversible cell voltage /V

References

[1] P. V. Aravind, *PhD Thesis*, University of Technology Delft, Delft, **2007**
[2] P. V. Aravind, T. Woudstra, N. Woudstra,H. Spliethoff, *J. Power Sources* **2009**, *190*, 461
[3] K. D. Panopoulos, L. E. Fryda, J. Karl, S. Poulou,E. Kakaras, *J. Power Sources* **2006**, *159*, 570
[4] C. Athanasiou, F. Coutelieris, E. Vakouftsi, V. Skoulou, E. Antonakou, G. Marnellos,A. Zabaniotou, *Int. J. Hydrogen Energy* **2007**, *32*, 337
[5] C. Athanasiou, E. Vakouftsi, F. A. Coutelieris, G. Marnellos,A. Zabaniotou, *Chem. Eng. J.* **2009**, *149*, 183
[6] T. Seitarides, C. Athanasiou,A. Zabaniotou, *Renew. Sustain. Energy Rev.* **2008**, *12*, 1251
[7] A. O. Omosun, A. Bauen, N. P. Brandon, C. S. Adjiman,D. Hart, *J. Power Sources* **2004**, *131*, 96
[8] L. Fryda, K. D. Panopoulos,E. Kakaras, *Energy Convers. Manage.* **2008**, *49*, 281
[9] T. Proell, C. Aichernig, R. Rauch,H. Hofbauer, *Proc. ASME Turbo Expo 2004: Power for Land, Sea, and Air,* (Eds. Vienna, Austria, **2004**, pp.
[10] M. Sucipta, S. Kimijima,K. Suzuki, *J. Power Sources* **2007**, *174*, 124
[11] R. Toonssen, N. Woudstra,A. H. M. Verkooijen, *Reference System for a Power Plant Based on Biomass Gasification and Sofc*, European Fuel Cell Forum, **2008**
[12] C.-X. Li, C.-J. Li,L.-J. Guo, *Int. J. Hydrogen Energy doi:10.1016/j.ijhydene.2009.05.033*,
[13] A. A. Peterson, F. Vogel, R. P. Lachance, M. Fröling, M. J. Antal,J. W. Tester, *Energy Environ. Sci.* **2008**, *1*, 32
[14] A. Kruse, *J. Supercrit. Fluids* **2009**, *47*, 391
[15] A. Kruse, *Biofuels, Bioprod. Biorefin.* **2008**, *2*, 415
[16] G. Brunner, *J. Supercrit. Fluids* **2009**, *47*, 373
[17] Y. J. Lu, L. J. Guo, C. M. Ji, X. M. Zhang, X. H. Hao,Q. H. Yan, *Int. J. Hydrogen Energy* **2006**, *31*, 822
[18] M. J. Antal, S. G. Allen, D. Schulman, X. Xu,R. J. Divilio, *Industrial & Engineering Chemistry Research* **2000**, *39*, 4040
[19] J. P. Ouweltjes, P. V. Aravind, N. Woudstra,G. Rietveld, *J. Fuel Cell Sci. Technol.* **2006**, *3*, 495
[20] *Cycle-Tempo*, TU Delft, version: 5.0, **2006**
[21] *Aspen Plus*, Aspen Techechnology Inc., version: 20.0.3595, **2006**
[22] ECN, *Phyllis, Database for Biomass and Waste*, ECN, http://www.ecn.nl/phyllis/, **2009**
[23] Y. Calzavara, C. Joussot-Dubien, G. Boissonnet,S. Sarrade, *Energy Convers. Manage.* **2005**, *46*, 615
[24] H. Tang,K. Kitagawa, *Chem. Eng. J.* **2005**, *106*, 261
[25] Y. Lu, L. Guo, X. Zhang,Q. Yan, *Chem. Eng. J.* **2007**, *131*, 233
[26] H. D. Baehr, *Thermodynamik; Eine Einführung in Die Grundlagen Und Ihre Technischen Anwendungen,* Springer, Berlin, **1984**,

Figure captions

Fig. 1 flow sheet of super critical water gasification
Fig. 2 flow sheet of the solid oxide fuel cell gas turbine hybrid system
Fig. 3 exergy flow diagrams for the three different systems
Fig. 4 heat-temperature diagrams for units 11, 14 & 73 for the different systems

Tables

Table 1 composition mixture of cow and pig manure[22]

Component	*wt% daf*	*mol% wet*
C	47.4	8.83
H	6.7	7.43
O	35.3	2.47
N	4.2	0.34
S	0.8	0.05
Cl	1.5	0.10
Ash	0	2.31
H_2O	0	78.48
LHV [kJ/kg]	19859	3960

Table 2 input values for hydrothermal gasification of the different systems

Unit	*Name*	*Case 1*	*Case 2*	*Case 3*
1	Source	p_{out}=1.01325, T_{out}=15, ϕ_m=0.2778	p_{out}=1.01325, T_{out}=15, ϕ_m=0.2778	p_{out}=1.01325, T_{out}=15, ϕ_m=0.2778
2	Sink/Source	p_{out}=350, T_{out}=21.1	p_{out}=350, T_{out}=21.1	p_{out}=250, T_{out}=19.32
3	Heat exchanger	Δp_h=6, Δp_l=6.1, $T_{out,h}$=195	Δp_h=6, Δp_l=6.1, $T_{out,h}$=195	Δp_h=5, Δp_l=5.1, $T_{out,h}$=140
4	Heat exchanger	Δp=0	Δp=0	Δp=0
5	Gasifier	Δp_1=0, $T_{in,2}$=400, p_{react}=343.9, T_{react}=408.49, $p_{out,2}$=343.9, $T_{out,2}$=408.49	Δp_1=0, $T_{in,2}$=500, p_{react}=343.9, T_{react}=500, $p_{out,2}$=343.9, $T_{out,2}$=500	Δp_1=0, $T_{in,2}$=600, p_{react}=343.9, T_{react}=600, $p_{out,2}$=343.9, $T_{out,2}$=600
6	Separator	Δp_1=6, Δp_2=6, ΔT_1=0, ΔT_2=0	Δp_1=6, Δp_2=6, ΔT_1=0, ΔT_2=0	Δp_1=5, Δp_2=5, ΔT_1=0, ΔT_2=0
7	Sink/Source	Δp=178.9, ΔH_{out}=0, $T_{out,est}$=187.5	Δp=178.9, ΔH_{out}=0, $T_{out,est}$=187.5	Δp=80.9, ΔH_{out}=0, $T_{out,est}$=150
8	Heat exchanger	Δp_h=3, Δp_l=0.01, $T_{out,h}$=25	Δp_h=3, Δp_l=0.01, $T_{out,h}$=25	Δp_h=3, Δp_l=0.01, $T_{out,h}$=25
9	Separator	Δp_1=100, Δp_2=100, ΔT_1=0, ΔT_2=0	Δp_1=100, Δp_2=100, ΔT_1=0, ΔT_2=0	Δp_1=50, Δp_2=50, ΔT_1=0, ΔT_2=0
10	Sink/Source	Δp=43, ΔH_{out}=0	Δp=43, ΔH_{out}=0	Δp=93.1, ΔH_{out}=0
11	Heat exchanger	Δp_h=0.001, Δp_l=0.1, $T_{out,l}$=400	Δp_h=0.001, Δp_l=0.1, $T_{out,l}$=400	Δp_h=0.001, Δp_l=0.1, $T_{out,l}$=404
12	Node			
13	Separator	Δp_1=0.2, Δp_2=0.2, ΔT_1=0, ΔT_2=0	Δp_1=0.2, Δp_2=0.2, ΔT_1=0, ΔT_2=0	Δp_1=0.2, Δp_2=0.2, ΔT_1=0, ΔT_2=0
14	Heat exchanger	Δp_h=0.01, Δp_l=0.042, $T_{out,h}$=859	Δp_h=0.001, Δp_l=0.042, $T_{out,h}$=862.5	Δp_h=0.001, Δp_l=0.1042, $T_{out,l}$=835.5
61	Sink/Source			
71	Separator	p_1=1.01325, p_2=1.01325, ΔT_1=24.4, ΔT_2=24.4	p_1=1.01325, p_2=1.01325, ΔT_1=24.4, ΔT_2=24.4	p_1=1.01325, p_2=1.01325, ΔT_1=24.4, ΔT_2=24.4
72	Combustor	p_{out}=1.016, λ=1.3, T_{react}=1000, p_{react}=1.01325	p_{out}=1.016, λ=1.3, T_{react}=1000, p_{react}=1.01325	p_{out}=1.016, λ=1.3, T_{react}=1000, p_{react}=1.01325
73	Heat exchanger	Δp_h=0.001, Δp_l=0, $T_{out,l}$=400	Δp_h=0.001, Δp_l=0, $T_{out,l}$=400	Δp_h=0.001, Δp_l=0, $T_{out,l}$=404
81	Sink/Source			
91	Sink/Source			
101	Sink/Source	p_{out}=1.01325, T_{in}=20, T_{out}=15	p_{out}=1.01325, T_{in}=20, T_{out}=15	p_{out}=1.01325, T_{in}=20, T_{out}=15
201	Sink/Source	p_{out}=1.01325, T_{out}=15	p_{out}=1.01325, T_{out}=15	p_{out}=1.01325, T_{out}=15
202	Node	Δp=0	Δp=0	Δp=0
301	Sink/Source	p_{out}=6.8, T_{out}=15, ϕ_m=0.0078	p_{out}=6.8, T_{out}=15, ϕ_m=0.005	p_{out}=6.8, T_{out}=15, ϕ_m=0.005

Table 3 input for the SOFC-GT hybrid system coupled to the hydrothermal gasification

Unit	*Name*	*All cases*
15	Node	$\Delta p=0$
16	Fuel cell	$\Delta p_{an}=0.2$, $\Delta p_{cat}=0.2$, $T_{in,an}=900$, $T_{in,cat}=900$, $T_{out}=1000$, $p_{fc}=6.5$, $T_{fc}=950$, $p_{react}=6.5$, $T_{react}=950$, $U_f=0.85$, DCAC=0.97, R_{eq}=5e-5, i=2500
17	Node	
18	Combustor	$\Delta p=0.5$, $T_{react}=1000$, $p_{react}=6.4$
19	Turbine	$\eta_i=0.80$
20	Heat exchanger	$\Delta p_h=0.001$, $\Delta p_l=0.2$, $\Delta T_h=30$
21	Stack	$p_{in}=1.01325$
22	Node	$\Delta p=0$
23	Heat sink	$\Delta p=0$, $T_{out}=110$
252	Compressor	PR=6.67, $\eta_i=0.80$
253	Node	$\Delta p=0$
254	Node	
501	Compressor	$\eta_i=0.70$
551	Compressor	$\eta_i=0.70$
G	Generator	$\eta=0.97$

Table 4 chemical composition of the environment[26]

Component	*Molar fraction [%]*
Ar	0.91
CO_2	0.03
H_2O	1.68
N_2	76.78
O_2	20.60

Table 5 composition in mole% of the fluid in different pipes of the system

Component	*Case 1*			*Case 2*			*Case 3*		
Pipe number (Figure 1)	10	11	16	10	11	16	10	11	16
Mass flow / kg s^{-1}	0.26	0.02	0.03	0.26	0.03	0.03	0.26	0.02	0.03
Temperature / K	298	298	1132	298	298	1136	298	298	1109
Pressure / bar	150.0	50.0	6.6	150.0	50.0	6.6	150.0	100.0	6.6
H_2	0.95	10.69	7.62	2.39	23.02	18.95	5.86	44.99	38.12
CH_4	5.60	59.57	42.49	5.19	47.89	39.40	4.19	30.57	25.90
CO	0.02	0.06	0.04	0.03	0.26	0.22	0.15	1.17	0.99
CO_2	4.79	25.07	17.88	5.10	24.92	20.51	5.79	20.18	17.10
H_2S	0.07	0.17	0.00	0.07	0.17	0.00	0.07	0.12	0.00
HCl	0.09	0.06	0.00	0.09	0.05	0.00	0.09	0.04	0.00
N_2	0.37	4.26	3.03	0.37	3.59	2.96	0.36	2.84	2.41
NH_3	0.02	0.01	0.00	0.02	0.01	0.01	0.03	0.01	0.01
H_2O	88.09	0.11	28.94	86.74	0.09	17.95	83.46	0.08	15.46

Table 6 separation factors for the two flashes in the different systems

	Case 1		*Case 2*		*Case 3*	
	Flash 1	Flash 2	Flash 1	Flash 2	Flash 1	Flash 2
Pressure / bar	50	1.01	50	1.01	100	1.01
Temperature / K	298	298	298	298	298	298
CH_4 / mole%	15.17	0.68	12.84	0.72	19.04	0.44
CO / mole%	0.00	0.00	8.73	0.00	14.35	1.09
CO_2 / mole%	58.26	6.52	53.83	6.66	61.36	4.48
H_2 / mole%	10.72	0.24	8.86	0.34	14.83	0.22
H_2O / mole%	99.99	99.86	99.99	99.87	99.99	99.80
H_2S / mole%	78.93	17.52	75.95	17.87	79.93	12.55
HCl / mole%	95.00	75.00	95.00	75.00	95.00	75.00
N_2 / mole%	9.33	0.71	7.79	0.00	12.53	0.00
NH_3 / mole%	97.90	74.54	97.32	75.23	97.66	66.40

Table 7 results of the SOFC/GT for the different cases

	Case 1	*Case 2*	*Case 3*
Air input / kg s^{-1}	0.31	0.33	0.37
Cell voltage / V	0.816	0.821	0.810
Active cell area / m^2	180.4	185.3	176.5
Anode recycle ratio / %	19.8	18.8	29.0
Cathode recycle ratio / %	53.7	54.7	60.6
Turbine inlet temperature / K	1462	1458	1414
Turbine outlet temperature / K	1084	1079	1042
Pressure ratio	6.7	6.7	6.7

Table 8 overview of the performance of the different systems

	Case 1		*Case 2*		*Case 3*	
	Energy / kW	Exergy / kW	Energy / kW	Exergy / kW	Energy / kW	Exergy /kW
Fuel input	830.72	841.85	830.72	841.85	830.72	841.85
Delivered power						
Fuel cell	356.94	356.94	368.88	368.88	346.58	346.58
Generator	87.63	87.63	92.81	92.81	94.58	94.58
Gross power	**444.57**	**444.57**	**461.68**	**461.68**	**441.16**	**441.16**
Auxiliary power consumption						
Aux power	25.00	25.00	25.80	25.80	23.90	23.90
Delivered power						
Net power	**419.57**	**419.57**	**435.88**	**435.88**	**417.26**	**417.26**
Total power	**543.78**	**473.55**	**556.20**	**487.00**	**575.01**	**487.31**
Efficiencies						
Gross el. eff. / %	53.52	52.81	55.58	54.84	53.11	52.40
Net el. eff. / %	50.51	49.84	52.47	51.78	50.23	49.57

Table 9 the units included in the different system sections as indicated in Fig. 3

System section	*Unit number in Fig. 1 or Fig. 2*
Gasifier	2, 3, 4, 5, 6, 7, 8, 9, 10, 71, 72, 101, 202
Cleaning	11, 12, 13, 14, 73
Fuel cell (FC)	15, 16, 17, 253, 254, 501, 551
Gas turbine (GT)	18, 19, 20, 22, 23, 252

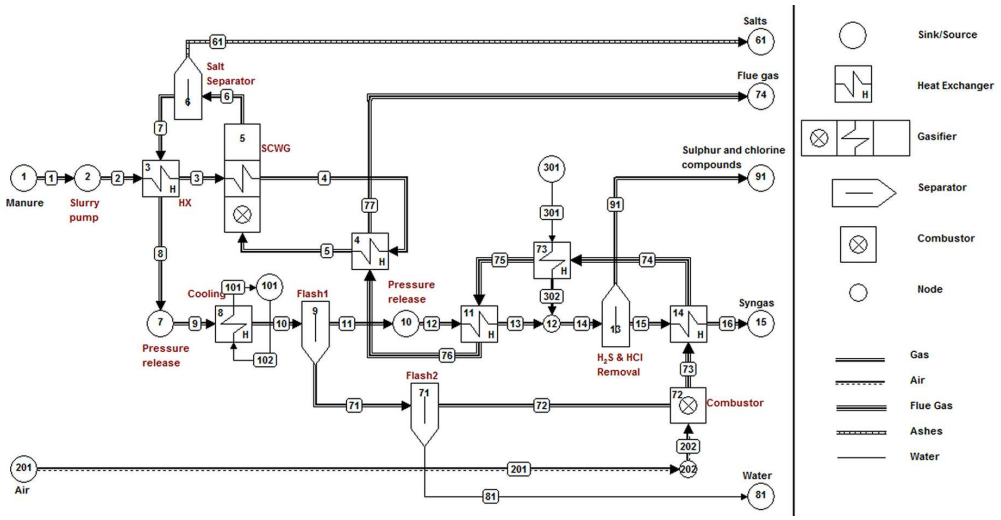

Fig. 1 flow sheet of super critical water gasification
77x39mm (600 x 600 DPI)

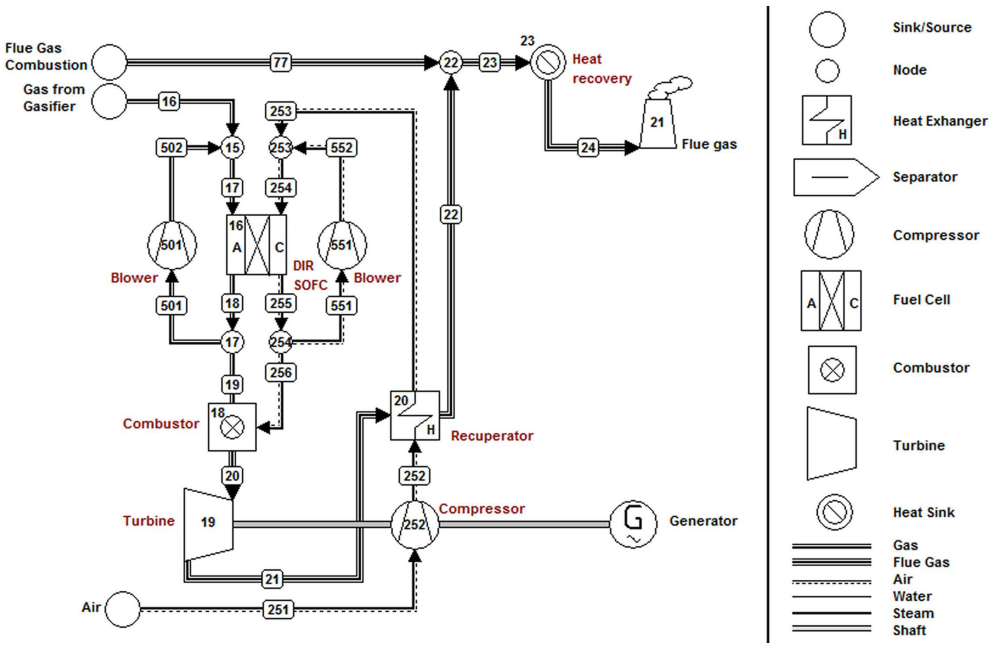

Fig. 2 flow sheet of the solid oxide fuel cell gas turbine hybrid system
96x61mm (600 x 600 DPI)

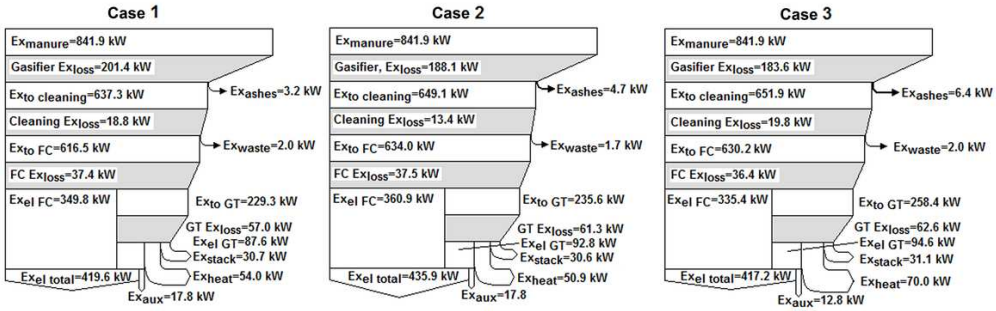

Fig. 3 exergy flow diagrams for the three different systems
49x15mm (600 x 600 DPI)

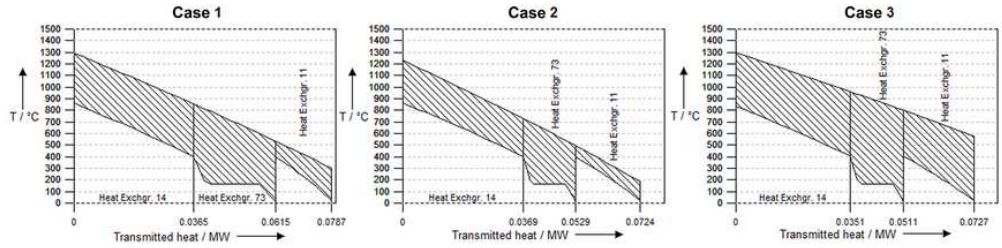

Fig. 4 heat-temperature diagrams for units 11, 14 & 73 for the different systems
36x8mm (600 x 600 DPI)